Jour. Korean Inst. Mining Geol.
Vol. 25, No. 4, p. 447-461, 1992.

Petrology of Jurassic Granitoids in the Hamyang-Geochang Area, Korea

Cheol-Lag Lee*, Yoon-Jong Lee and Masao Hayashi*****

ABSTRACT: The Jurassic granitoids in the study area are divided into the "Gneissose granodiorite" and the "Daebo granodiorite" (1 : 250,000 Jeonju Geological map, 1973). The term of Geochang granodiorite was used in this study instead of "Daebo granodiorite". These granitoids were studied in terms of microscopic observation, petrochemistry, and zircon morphology.

The granitoids are mostly granodiorite. Two kinds of progressive variation can also be recognized in the modal quartz~alkali feldspar~plagioclase triangular diagram; the Gneissose granodiorite is in accordance with the trondhjemitic (low *k*) trend, and the Geochang granodiorite with the granodioritic trend (medium *k*). The granitoids belong to the calc-alkaline series, and are classified into the I-type (magnetite series).

Plagioclase ($An_{25.1}$~$An_{30.9}$) in the granitoids shows generally an oligoclase composition. Biotite has a wider range in (Si, Al) solution than in (Fe, Mg) solid solution. Hornblende occurs in a few thin sections of the Geochang granodiorite, and is plotted in the tschermakite field. The zircon prism shows a long variation between the {110} dominant type and the {100} dominant type in the Geochang granodiorite, but only the {110}={100} type in the Gneissose granodiorite. However, zircon crystals in the granitoids are mostly crystallized in a low-to-medium temperature magma. In the PPEF (Prism- Pyramid-Elongation-Flatness) diagram, the Gneissose granodiorite shows a closed scissors type, the Geochang granodiorite, a opened scissors type. It indicates that the Geochang granodiorite might originate from the mixed magma with crustal materials or pre-existed residual magma which had formed the Gneissose granodiorite.

INTRODUCTION

In the Mesozoic period several times of orogenesis in the Korean peninsula have been recognized: the Songlim disturbance, the Daebo orogeny, and the Bulgugsa disturbance. Magmatism in the Daebo orogeny period seems to have occurred twice (Park and Do, 1973). But recently, there was a debate about the "Daebo orogeny and its problems" in the petrological subcommittee of the Geological Society of Korea (1987). The major point of the debate was chiefly that the petrogenetic relation of Daebo granodiorite and Daebo orogeny is not obvious. It is questionable that the Daebo granodiorite is related at all to the Daebo orogeny as known generally. The magmatic origin of Mesozoic granitoids is also in dispute between those who claim the same origin and others who favor a different one. Much more data and the evaluation of each interpretation will be necessary.

* Taegu Education and Science Research Institute, Taegu 706-040, Korea.
** Department of Earth Science, Kyungpook National University, Taegu 702-701, Korea.
*** Kyushu Sangyo University, 813, Japan.

GENERAL GEOLOGY

The study area is located in the central part of the "Ryongnam massif" elongated to the NE-SW trend across the Korean peninsula (Fig. 1).

Parts of the Sobaegsan gneiss complex is exposed as a pre-Cambrian basement in the northern part of the study area. The belt-shaped Jirisan migmatitic gneiss is sandwiched among the Mesozoic granitoids at intervals. The gneiss complex is composed of migmatitic gneiss, porphyroblastic gneiss, banded gneiss, and biotite schist, which shows a gradational boundary with each other in the field. In the southern part, anorthosite of unknown age is intruded by the Mesozoic granitoids.

Several magmatisms in the Jurassic and the Cretaceous period have made up the acidic granitoids in the area, but the age of the intermediate and basic rock is not known yet. The acidic granitoids with or without foliation have been used under the name of "Gneissose granodiorite (Jgng)" and "Daebo granodiorite (Jg)" respectively (1 : 250, 000 Jeonju Geological map, 1973). But it is especially difficult to fix the boundary of the presence and the absence of foliation in the field, while the

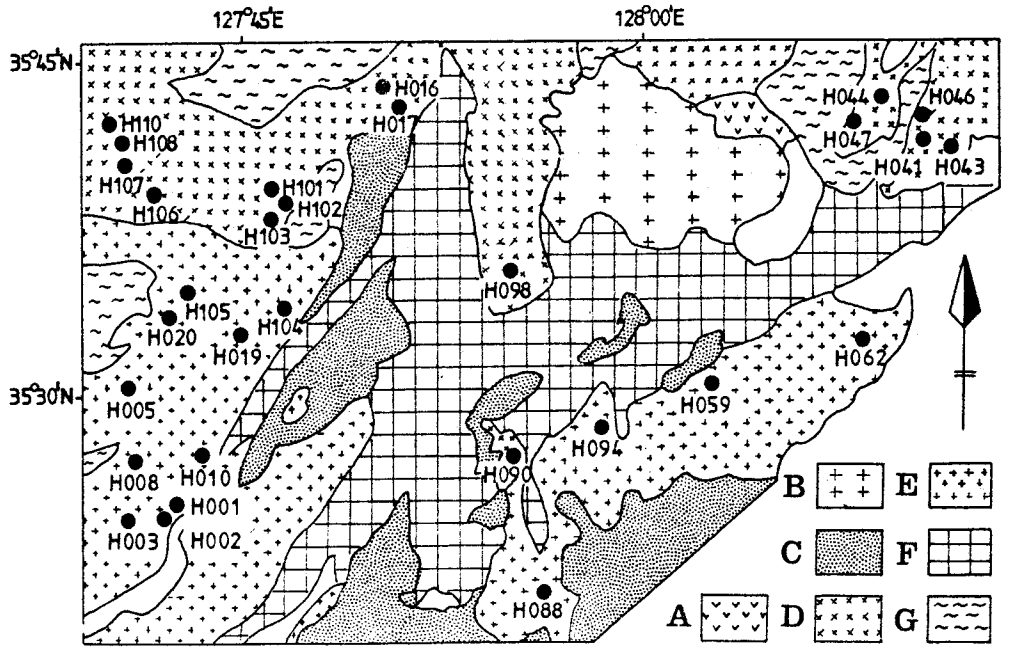

Fig. 1. Geologic map of the study area and sampling localities. A; Intermediate volcanic rocks, B; Gajo granodiorite, C; Intermediate and basic plutonic rocks, D; Geochang granodiorite, E; Gneissose granodiorite, F; Jirisan gneiss complex, and G; Sobaegsan gneiss complex.

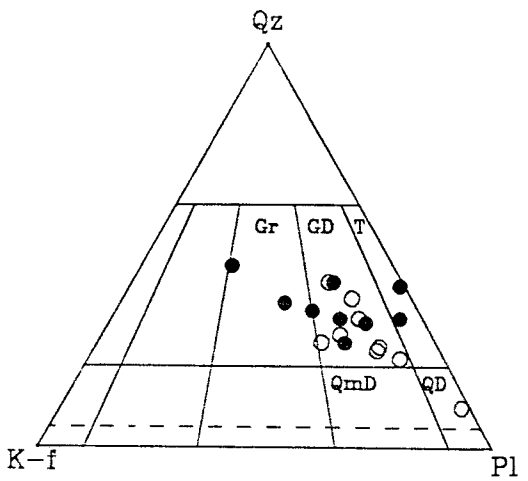

Fig. 2. Modal QAP triangular diagram. Filled circle; the Gneissose granodiorite and Open circle; the Geochang granodiorite.

intermediate and basic rocks of unknown age show a sharp boundary with the pre-Cambrian basement. The term of Geochang granodiorite (Gc) was used in this study instead of "Daebo granodiorite (Jg)".

This study deals mainly with the Jurassic acidic granitoids in the area.

PETROGRAPHY AND MINERALOGY

The modal compositions of the granitoids are presented in Table 1, and are plotted in Fig. 2.

The Gneissose granodiorite is scattered transversely from tonalite to adamellite, while the Geochang granodiorite stretches through quartz diorite and granodiorite (Fig. 2a). For all that, the two granitoids are mostly plotted within a limited area, and are classified as granodiorite. Two progressive variation trends can be found in modal composition (Fig. 2b). The plots of the Gneissose granodiorite are in accordance with the trondhjemitic (low *k*) trend of calc-alkaline magma (Lameyre and Bowden, 1982). But the Geochang granodiorite is traced along the granodioritic trend (medium *k*) of the magma. The trondhjemite is primarily composed of sodic plagioclase. The change in plagioclase content of the Geochang granodiorite is especially noted.

Plagioclase

Plagioclase is anhedral to subhedral in form, showing weak or absent zonal structure, in

Table 1. Modal analyses of the granitic rocks in the study area.

Rx	Gneissose granodiorite (HGn)								
Sp	H1-1	H1-2	H5	H8	H10	H19	H59	H8	H104
Qz	32.4	36.1	26.8	27.4	32.9	31.4	30.5	24.6	40.4
Pl	49.2	39.2	46.9	53.5	32.8	38.9	46.5	51.9	18.5
Af	0.2	13.5	11.8	4.1	26.7	21.8	17,3	19.4	31.8
Ne	0.7	–	0.3	0.1	–	–	0.5	0.2	–
Bt	15.1	9.7	11.8	12.2	6.4	6.7	3.7	1.9	8.1
Mu	–	–	–	0.5	0.2	0.2	0.1	0.1	–
Hb	–	–	–	–	–	–	–	0.1	–
Zr	0.6	0.8	0.6	0.3	0.1	0.2	0.3	0.4	0.3
Ap	0.3	0.1	0.3	0.2	0.2	0.1	0.1	0.3	0.2
Sp	1.2	0.1	0.5	0.7	0.5	–	–	0.2	0.6
Op	0.1	0.6	0.8	0.7	0.1	0.7	1.1	0.8	–
Al	–	–	0.2	0.3	0.1	–	–	–	0.2
Ep	–	–	–	0.1	–	–	–	–	–
Ca	–	–	–	–	–	–	–	–	–
Py	–	–	–	–	–	–	–	–	–
CI	17.0	11.2	13.9	14.8	7.4	7.8	5.2	3.5	9.2
Rx	Geochang granodiorite (Gc)								
Sp	H17	H41	H43	H46	H90	H102	H103	H106	H108	H110
Qz	20.2	35.0	37.5	7.2	16.8	27.5	25.0	30.6	23.3	22.4
Pl	49,2	45.7	38.9	66.8	52.5	47.1	46.2	44.9	43.6	43.0
Af	10.5	13.0	14.5	1.5	7.4	12.2	17.7	15.8	22.8	28.6
Ne	–	–	–	–	–	0.8	0.4	–	–	
Bt	12.6	6.0	6.2	14.2	10.9	10.2	8.7	6.9	8.3	4.4
Mu	0.5	–	–	0.1	–	0.5	0.1	–	0.3	
Hb	2.3	0.3	0.6	5.0	0.3	–	–	–	–	
Zr	0.4	0.1	0.3	0.6	1.0	0.6	0.6	0.5	1.3	0.5
Ap	0.4	–	0.2	0.7	0.8	0.4	0.3	0.4	0.4	0.2
Sp	1.2	–	0.4	1.0	0.2	–	–	0.1	–	–
Op	0.5	0.3	1.3	2.0	1.5	0.7	0.9	0.8	0.3	0.6
Al	–	–	0.1	–	–	–	–	–	0.1	–
Ep	2.1	–	–	0.6	–	–	–	–	–	0.1
Ca	–	–	–	0.1	8.6	–	–	–	–	–
Py	–	–	–	0.3	–	–	–	–	–	–
CI	19.6	6.7	8.9	38.1	13.9	12.0	10.3	8.3	10.0	5.9

accordance with the albite twin law, but it is often found with pericline and carlsbad-albite twin law. In some thin sections, plagioclase is rarely penetrated into the crystal by mottled muscovite. The albite composition plane (010) of the Geochang granodiorite is rarely bent, with biotite cleavage. It is often sericited near the core or most of the crystal, except for the albite rim. The albite end of the plagioclase series is relatively resistant to alteration. Partial replacement of plagioclase by microcline is rarely encountered in a thin section of the Gneissose granodiorite (H088).

Gradation from the inner zone to the outer zone is mostly unclear, with weak zonal structure. Many of the crystals are relatively homogeneous. If cooling is continuous, without interruption or disturbance, then continuous normal zoning will be resulted. The normal zoning is found in the Geochang granodiorite more often than in the Gneissose granodiorite, although plagioclase in these granitoids has weak or absent zoning as a whole. This suggests that the cooling process of the Geochang granodiorite was probably longer and more continuous than the Gneissose granodiorite.

The plagioclases of the Gneissose granodiorite range in composition from An29.0 to An30.9, which

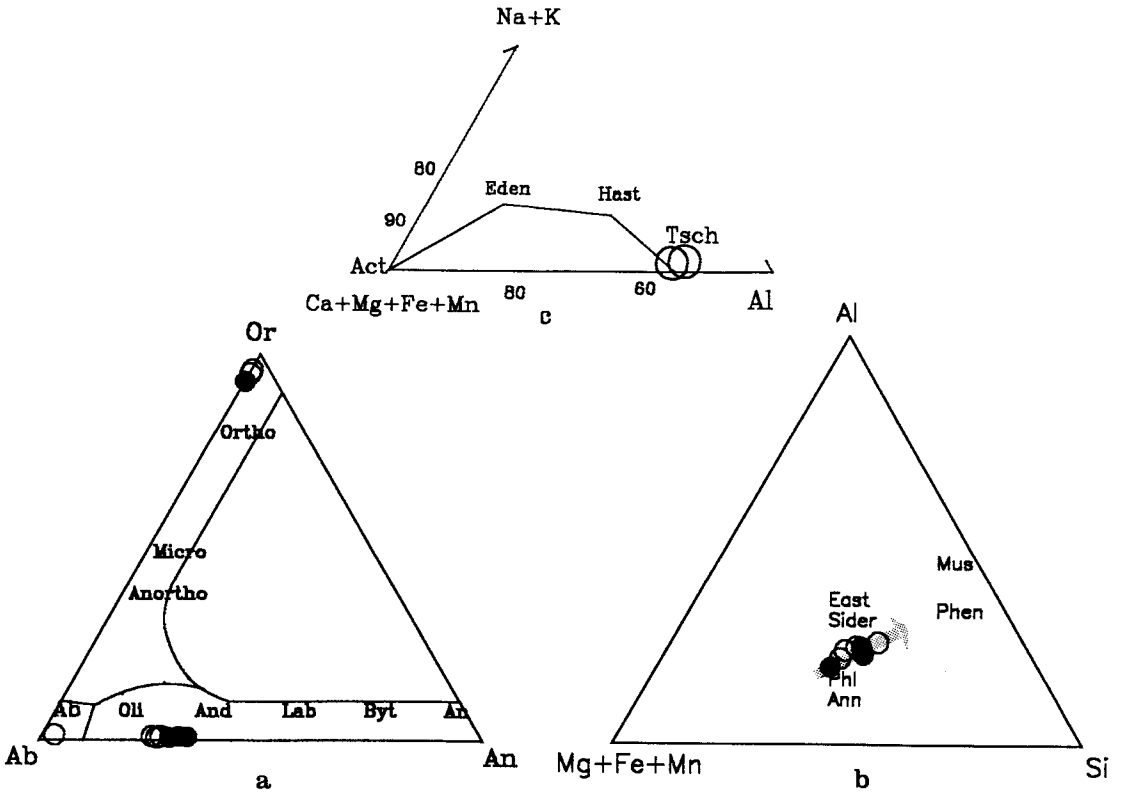

Fig. 3. Chemical composition of plagioclase and alkali feldspar (a), biotite (b) and hornblende (c). Symbols are the same as those in Fig.2.

is typical of oligoclase and andesine, whereas those of the Geochang granodiorite range from An2.7 to An26.9, which links to albite and oligoclase (Fig. 3a). The composition of plagioclase establishes that the plagioclases of the Geochang granodiorite were crystallized in a more sodic and lower-temperature melt than those of the Gneissose granodiorite.

Since the Geochang granodiorite is richer in mafic minerals and metallic elements than the Gneissose granodiorite, in spite of the formation temperature of the plagioclase is lower, there are two possible magma origins: either there were originally two types of magma, which were different both chemically and physically, or the Gneissose granodiorite was differentiated from the Geochang granodiorite by a comagma suit. If the former is true, the magma should show two distinct differentiation trends in modal and chemical composition. If the latter is true, the fractionation of water-rich magma might have continued at a slow cooling rate for a long time. And the fractionation of the Gneissose granodiorite might have lasted in the late fluids for a relatively short time. The former is supported by the mafic mineral contents, plagioclase composition, Fe content of biotite, and zircon morphology.

Potash Feldspar

Potash feldspar has mostly a microcline texture with cross-hatched twinning or string type, but often patch type perthite. Perthite is not found in some thin sections of the Gneissose granodiorite. It is thought to be splitted into two phases of orthoclase and albite by the recrystallization of an early formed perthite. In a thin section which does not contain any microclines, it is rarely found what is thought to be anorthoclase in the Geochang granodiorite (H 102) with near 50° of 2Vz.

The microcline has rarely a zonal structure due to variations in the soda content, and some inclusions are rarely arranged zonally (H110 of the Geochang granodiorite) on the microcline crystal. This zone of inclusions seems to denote that at least the later stages of crystallization of the feldspar have been

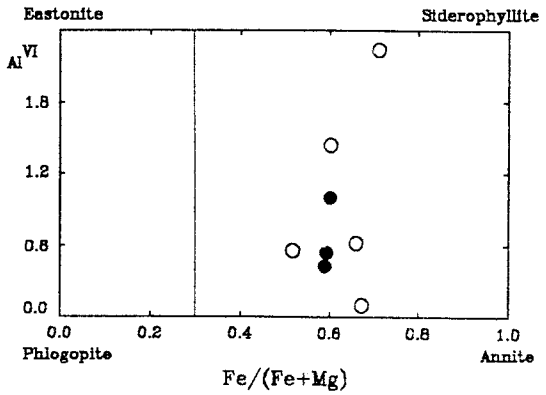

Fig. 4. Octahedral aluminum vs. Fe/ (Fe+Mg) ratio in biotites of the granitic rocks. Symbols are the same as those in Fig. 2.

intermittent or interrupted in a limited area (Moorhouse, 1959).

Biotite

Biotites of the Geochang granodiorite show mostly a mottled appearance, whereas the Gneissose granodiorite both a mottled appearance and a wavy extinction. Biotite shows a relatively weak pleochroism of pale green to yellowish brown. The biotite is fresh and/or partly altered into chlorite. The chloritization in the Gneissose granodiorite makes rapid progress. The biotites of the Gneissose granodiorite show also preferred orientation weakly under a microscope as well as in the field: both biaxial and uniaxial characteristics can be easily seen under a conoscope, but the biaxial is predominant. A dark brown to black radioactive halo is visible around the zircon and allanite in biotite.

It is generally thought that Fe in biotite increases, but the total Fe in the rock decreases with an increasing differentiation index (DI). In this study the biotite shows also an increase in Fe, Si, and Al, as well as a decrease in Mg and Mn, as the DI values increase from 65 (H90) to 84 (H110). There is no great difference in biotite composition between the Geochang and the Gneissose granodiorite, but the biotite of the Geochang granodiorite is slightly higher in Fe, and lower in Mg and Mn. This suggests that the Geochang granodiorite is later in intrusion than the Gneissose granodiorite, because an increase in Fe and a decrease in Mg is common for the late-formed biotites of any intrusion when compared with early-formed biotites from any other intrusion. The arrows in Fig. 3b show the direction of increasing DI and that of decreasing Mg and Mn.

Relationship of Al and Si, which is the (Al, Si) solution between Eastonite (Siderophyllite) and Phlogopite (Annite), is in Fig. 4. From the wide variation of Al in Fig. 4, it is assumed that the Al^{3+} chemistry is complicated in both the tetrahedral and the octahedral coordination.

The range of Fe/Fe+Mg ratio is small as compared with Al^{VI} in Fig. 4. The plots occupy the limited range of the (Fe, Mg) solid solution, that is 0.5 to 0.7. It may means that Fe^{2+} replaced Mg^{2+} restrictively. Fe^{2+} usually replaces Mg^{2+}, and Fe^{3+} replaces Al^{3+} in pyroxenes and amphiboles. Fe^{2+} occurs exclusively in octahedral coordination in micas (Wedepohl, 1978). As the fugacity of water and oxygen exceed critical values through the process of magma differentiation, MgO would precipitate largely as mica in the area. After that Mg^{2+} in mica would be replaced by Fe^{2+} between Phlogopite (Eastonite) and Annite (Siderophyllite).

Hornblende and Accessory Minerals

The Gneissose granodiorite does not contain any hornblende. Hornblende occurs in some limited sections of the Geochang granodiorite, and that is plotted as tschermakite (Fig. 3c).

Allanite, usually yellowish brown in color, is found in limited sections of the Gneissose granodiorite. The allanite has a distinctive zoning. Sphene is euhedral to subhedral, varies in size, and includes some opaque minerals thought to be ilmenite.

Zircon is euhedral, relatively small sized, and pale in color, compared with the crystals of other pre-Cambrian granitoids. The {100} and {110} prism used by Karakida (1963) is also distinguishable on thin sections. The development of the {110} prism in zircon crystals seems to be related to the amount of muscovite and myrmekite. But the quantitative relationship between the two has not been determined in this study.

ZIRCON MORPHOLOGY

Zircon crystals have some characteristic habits according to the physicochemical conditions of their formation. A quantitative observation of the habits has been applied to the interpretation of various petrogenetic problems.

Hayashi (1989) proposed four indexes to describe zircon crystal forms:

Table 2. Representative electron probe microanalyses of plagioclase and alkali feldspar in the granitic rocks. Pfg1 and Pfg2 were taken from Park et al., 1990.

	Plagioclase						Alkali feldspar				
Rock	Gneissose gd.(HGn)		Geochang gd.(Gc)				Gneissose gd.(HGn)			Geochang gd.(Gc)	
Sample	H105	Pfg2	H90	H102-1	H102-2	H103	H105	Pfg1	Pfg2	H90	H103
SiO_2	60.393	61.460	60.733	67.920	60.566	61.602	63.206	64.970	64.910	64.341	63.803
Al_2O_3	25.428	24.600	24.787	20.836	24.945	24.651	18.505	18.350	18.480	18.784	18.555
FeO*	–	0.030	–	–	–	–	–	0.030	0.010	0.071	–
MnO	0.022	–	–	0.020	0.061	–	–	–	–	0.092	–
MgO	0.011	–	–	0.033	0.006	–	0.008	–	–	0.002	0.012
CaO	6.191	6.380	5.484	0.588	5.636	5.315	0.021	–	0.010	–	0.019
Na_2O	8.278	7.800	8.405	11.537	8.344	8.674	0.685	0.400	0.430	0.571	0.426
K_2O	0.139	0.140	0.116	0.258	0.167	0.171	15.082	16.180	16.040	15.490	15.585
Total	100.461	100.410	99.524	101.193	99.726	100.413	97.508	99.930	99.880	99.351	98.400
	Numbers of ions on the basis of 8 oxygens										
Si	2.676	2.718	2.708	2.937	2.698	2.722	2.982	3.002	2.999	2.983	2.986
Al	1.328	1.282	1.303	1.062	1.310	1.284	1.029	1.000	1.006	1.027	1.023
Fe	–	0.001	–	–	–	–	–	0.001	–	0.003	–
Mn	0.001	–	–	0.001	0.002	–	–	–	–	0.004	–
Mg	0.001	–	–	0.002	–	–	0.001	–	–	–	0.001
Ca	0.294	0.302	0.262	0.027	0.269	0.252	0.001	–	–	–	0.001
Na	0.711	0.669	0.727	0.967	0.721	0.743	0.063	0.036	0.039	0.051	0.039
K	0.008	0.008	0.007	0.014	0.010	0.010	0.908	0.954	0.945	0.916	0.930
	Mole proportion (%)										
Ab	70.2	68.3	73.0	95.9	72.1	74.0	6.5	3.6	3.9	5.3	4.0
Or	0.8	0.8	0.7	1.4	1.0	0.9	93.4	96.4	96.0	94.7	95.9
An	29.0	30.9	26.3	2.7	26.9	25.1	0.1	0.0	0.1	0.0	0.1
	Ol	And	Ol	Ab	Ol	Ol					

Asbreviations: Gc; Geochang granodiorite, HGn; Gneissose granodiorite, gd.; granodiorite, Ab; albite, Ol; oligoclase, and And; andesine.

$$FI = T_{100}/W_{100} = T_{110}/W_{110}$$
$$EI = H_{PR}/(H+0.5T_{100}+0.5W_{100}) = H_{PR}/(H+0.5T_{110}+0.5W_{110})$$
$$PI = (T_{100}-W_{100}+2W_m)/T_{100}+0.41W_{100}+0.59W_m) = (W_{110}-W_m)/(0.71T_{110}+0.29W_{110}+0.42W_m)$$
$$PY = H_{py}/0.68\ (T_{100}+W_{100}) = H_{py}/0.72\ (T_{110}+W_{110})$$

The prism and the pyramid indices are related to the temperature and the chemical composition of the magma. Zircon morphology in this study is briefly dealt with using these two indices. The detailed zircon morphology will be reported in a separate paper.

The mean prism index of the Geochang granodiorite generally shows a wide range between 0.30, {110} dominant type, and 0.55, {100} dominant type in the PPEF diagram (Fig. 5). That of the Gneissose granodiorite is in a relatively narrow range between 0.48 and 0.55. Especially the Geochang granodiorite shows the opened scissors type in the PPEF diagram, which is largely splitted into two group. The Gneissose granodiorite shows the closed scissors type. But, as a whole, it can be said that the Geochang granodiorite is chiefly plotted in the {110} dominant type field, whereas that of the Gneissose granodiorite is concentrated near 0.50, {110}={100} type. The {110} prism of zircon is well developed in low temperature (about 550°C) magma, and {100} prism is formed at high temperature (>900°C) (Pupin, 1980; Hayashi, 1990). In water-rich magma, zircon crystallization begins early in the magmatic period and continues up to the end, whereas zircon crystallizes during an early magmatic period in water-poor magmas (Pupin, 1980). From the above results, the Geochang granodiorite probably originated from water-rich magma, and might have undergone a long and continuous crystallizing process in high to low temperature conditions, but

Table 3. Representative electron probe microanalyses of biotite and hornblende in the granitic rocks. Pfg1 and Pfg2 were taken from Park et al., 1990.

	Biotite								Hornblende	
Rock	Gneissose gd. (HGn)			Geochang gd. (Gc)					Gneissose gd. (HGn)	
Sample	H105	Pfg1	Pfg2	H90	H102	H103-1	H103-2	H110	H41	H90
SiO_2	36.145	36.580	36.480	33.704	33.241	35.379	34.945	29.825	36.741	37.644
Al_2O_3	17.910	15.950	15.890	16.292	17.690	17.445	17.926	14.715	22.865	22.975
FeO*	24.190	21.740	22.020	25.057	30.433	27.839	29.364	16.578	15.428	14.899
MnO	0.424	0.400	0.380	0.394	0.274	0.333	0.293	0.295	0.351	0.270
MgO	8.112	8.370	8.630	11.798	7.917	6.813	6.005	5.526	0.017	0.040
CaO	0.064	0.000	0.000	0.088	0.089	0.117	0.038	0.020	21.501	21.567
Na_2O	0.066	0.070	0.110	0.047	0.035	0.094	0.127	0.132	–	–
K_2O	9.218	9.730	9.580	5.429	6.015	8.319	9.679	7.037	0.033	0.020
TiO_2	1.827	2.650	2.210	1.508	1.546	1.957	1.961	1.579	0.062	0.023
Total	97.955	95.490	95.300	94.317	97.241	98.296	100.339	75.707	96.997	97.438
	Numbers of ions on the basis of 22 oxygens								Numbers of ions on the basis of 23 oxygens	
Si	5.686	5.643	5.644	5.454	5.299	5.123	6.380	5.969	5.457	5.542
Al(IV)	2.314	2.357	2.356	2.546	2.701	2.877	1.620	2.031	2.543	2.458
Al(VI)	1.007	0.543	0.541	0.562	0.623	0.100	2.238	1.440	1.460	1.529
Fe	2.864	2.805	2.849	3.052	3.651	3.034	4.034	2.497	1.724	1.651
Mn	0.056	0.052	0.050	0.054	0.037	0.041	0.045	0.050	0.044	0.034
Mg	1.903	1.925	1.991	2.846	1.881	1.471	1.634	1.649	0.004	0.009
Ca	0.011	0.000	0.000	0.015	0.015	0.018	0.007	0.004	3.422	3.402
Na	0.020	0.021	0.033	0.015	0.011	0.027	0.045	0.051	–	–
K	1.850	1.915	1.891	1.121	1.223	1.537	2.254	1.797	0.006	0.004
Ti	0.216	0.307	0.257	0.183	0.185	0.213	0.269	0.238	0.007	0.003

Abbreviations: Gc; Geochang granodiorite, HGn; Gneissose granodiorite, and gd.; granodiorite.

Table 4. Morphological data of zircon crystals from the granitic rocks in the study area.

Sample No.	Width (mm)	Height (mm)	Flatness Index	Elongation Index	Prism Index	Pyramid Index
Gc-H016	0.063± 0.015	0.159± 0.055	0.89± 0.08	0.41± 0.08	0.38± 0.24	0.39± 0.07
Gc-H098	0.088± 0.021	0.224± 0.065	0.89± 0.07	0.39± 0.11	0.55± 0.28	0.42± 0.07
Gc-H107	0.058± 0.015	0.149± 0.033	0.84± 0.09	0.32± 0.09	0.30± 0.23	0.48± 0.06
HGn-H005	0.099± 0.029	0.241± 0.054	0.88± 0.06	0.40± 0.11	0.55± 0.17	0.40± 0.07
HGn-H008	0.093± 0.017	0.260± 0.033	0.87± 0.08	0.44± 0.08	0.48± 0.14	0.43± 0.05
HGn-H020	0.078± 0.014	0.215± 0.040	0.87± 0.08	0.41± 0.09	0.49± 0.17	0.45± 0.05

Abbreviations: Gc; Geochang granodiorite and HGn; Gneissose granodiorite.

mainly crystallized in a low temperature melt. The {110} prism is also more developed as magma is differentiated (Lee, 1990). The low prism index of the Geochang granodiorite, in spite of its higher content of mafic minerals, supports the existence of two different kinds of magma or the mixing between the residual magma and another source magma in the area, according to the results of modal analysis, plagioclase composition, and Fe content in biotite.

The relative development of the zircon pyramid depends on the chemistry of zircon (Caruba et al., 1974). In this study, the mean pyramid index of the zircon is within the range from 0.43 to 0.45 in the Gneissose granodiorite, 0.39 to 0.48 in the Geochang granodiorite. The Gneissose granodiorite has {101}= {211} pyramid, whereas the Geochang granodiorite has both of {101} dominant and {211} dominant in their pyramid forms.

PETROCHEMISTRY

The results of the bulk chemical analyses of twenty

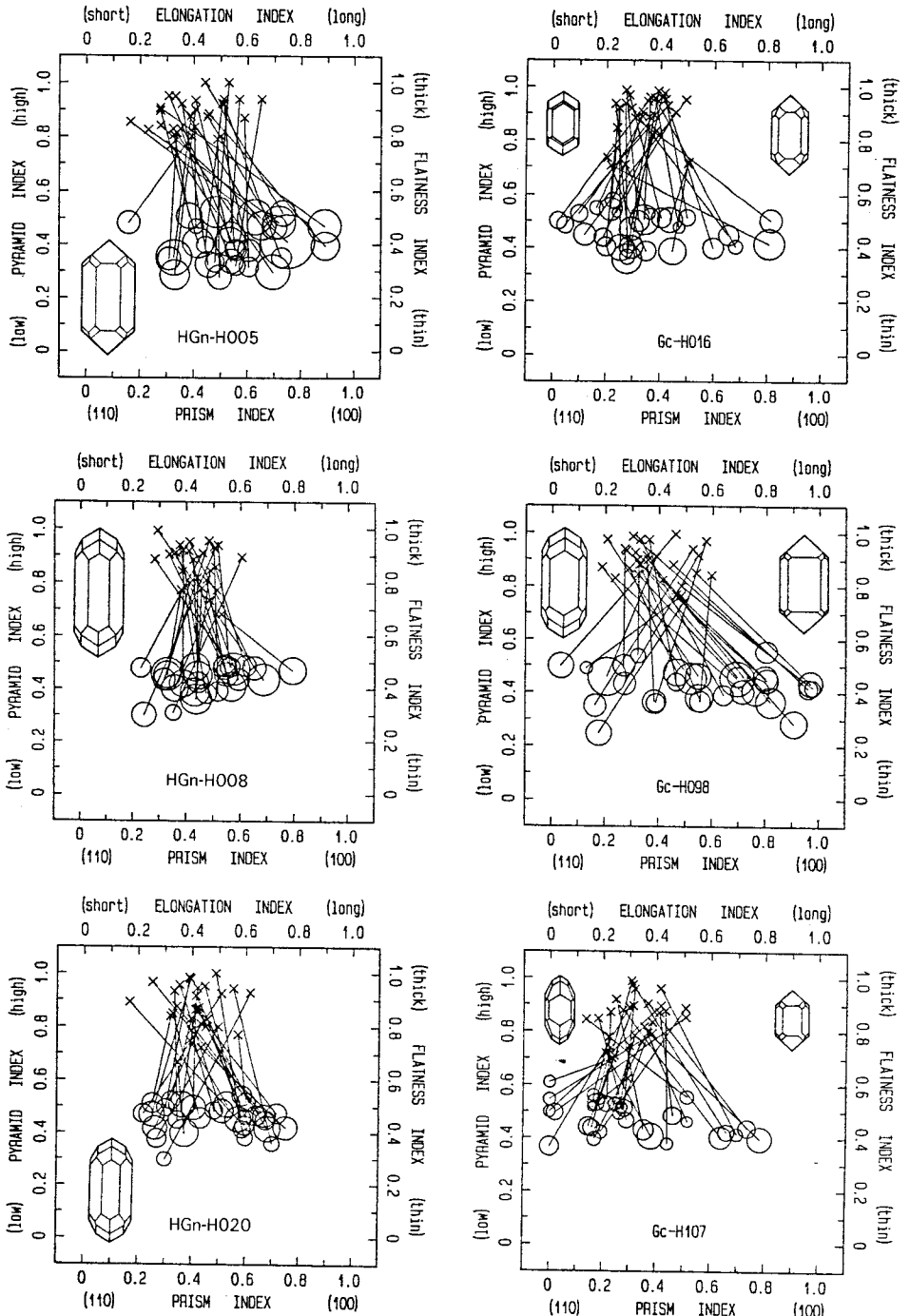

Fig. 5. PPEF diagrams of zircon crystals in the granitic rocks. The circles show the relation between prism and pyramid indexes, the crosses, that between flatness and elongation indexes. The straight lines link the two symbols for each crystal. The diameter of the circles is propotional to the crystal width (W).

five samples, obtained using an ICP spectrometer (Phillips PV8060) at London University and the conventional wet method*[1], are listed in Table 5 with *[1]; SiO_2, FeO, H_2O (+), and H_2O (−).

Table 5. Major element oxides and CIPW normative minerals of the granitic rocks.

Rock	Gneissose granodiorite (HGn)													
Sample	H1-1	H1-2	H3	H5	H8	H10	H19	H59	H62	H84	H88	H94	H104	H105
SiO_2	70.79	69.21	74.61	66.55	67.93	71.92	71.38	73.18	74.41	71.90	70.63	74.65	68.10	67.14
TiO_2	0.49	0.48	0.17	0.57	0.59	0.30	0.22	0.23	0.21	0.09	0.13	0.12	0.35	0.51
Al_2O_3	15.23	15.57	14.23	15.51	16.69	15.37	14.90	14.31	13.74	15.34	16.15	13.49	15.18	16.02
Fe_2O_3	0.16	0.82	0.80	0.87	132	0.69	0.85	1.30	1.27	0.58	0.85	0.89	0.63	1.26
FeO	2.80	2.10	0.85	2.20	2.32	1.50	1.51	1.18	1.05	0.75	0.87	0.91	1.69	2.32
MnO	0.04	0.04	0.02	0.04	0.06	0.04	0.03	0.06	0.06	0.03	0.03	0.06	0.04	0.09
MgO	0.75	0.83	0.21	0.88	1.07	0.52	0.32	0.43	0.50	0.12	0.18	0.14	0.64	1.10
CaO	2.49	2.04	1.10	2.18	2.86	2.07	1.32	1.46	0.27	1.48	1.50	0.55	2.16	2.75
Na_2O	3.38	3.14	3.01	3.18	3.81	3.54	3.30	3.68	3.90	4.93	5.07	3.51	3.22	3.74
K_2O	3.51	5.15	5.12	4.79	3.02	4.28	5.09	4.41	4.26	3.24	3.23	4.35	4.70	2.80
P_2O_5	0.12	0.13	0.06	0.15	0.15	0.09	0.07	0.08	0.06	0.05	0.06	0.03	0.10	0.15
H_2O^-	0.10	0.15	0.24	0.06	0.15	0.08	0.49	0.01	0.12	0.07	0.15	0.07	0.05	0.11
H_2O^+	0.40	0.49	0.09	0.44	0.57	0.21	0.22	0.04	0.50	0.62	0.62	0.53	0.30	0.37
Total	100.26	100.15	100.51	97.42	100.54	100.61	99.70	100.37	100.35	99.20	99.47	99.30	97.16	98.36
Qz	29.65	24.89	34.73	23.06	25.88	29.21	28.81	31.00	33.99	27.27	25.15	35.92	25.15	26.42
Or	20.74	30.42	30.25	28.30	17.84	25.28	30.07	26.05	25.17	19.14	19.08	25.70	27.77	16.54
Ab	28.59	26.56	25.46	26.90	32.22	29.94	27.91	31.12	32.98	41.70	42.88	29.69	27.23	31.63
An	11.57	9.28	5.07	9.84	13.22	9.69	6.09	6.72	0.95	7.02	7.05	2.53	10.07	12.67
Co	1.63	1.43	1.88	1.49	2.31	1.37	1.73	1.02	2.37	1.15	1.73	2.08	1.11	2.20
Hy En	1.87	2.07	0.52	2.19	2.66	1.29	0.80	1.07	1.24	0.30	0.45	0.35	1.59	2.74
Fs	4.27	2.46	0.66	2.45	2.31	1.76	1.76	0.82	0.64	0.81	0.74	0.85	2.08	2.54
Il	0.93	0.91	0.32	1.08	1.12	0.57	0.42	0.44	0.40	0.17	0.25	0.23	0.66	0.97
Mt	0.23	1.19	1.16	1.26	1.91	1.00	1.23	1.88	1.84	1.84	1.23	1.29	0.91	1.83
Ap	0.28	0.30	0.14	0.35	0.35	0.21	0.16	0.18	0.14	0.12	0.14	0.07	0.23	0.35
D.I.	78.98	81.87	90.44	78.26	75.94	84.43	86.79	88.17	91.14	88.11	87.11	91.31	80.15	74.59

Rock	Geochang granodiorite(Gc)										
Sample	H17	H41	H44	H46	H47	H90	H101-2	H102	H103	H108	H110
SiO_2	67.51	69.87	69.63	57.98	68.26	61.72	71.06	68.33	67.89	70.81	70.59
TiO_2	0.33	0.28	0.34	0.71	0.46	0.75	0.15	0.43	0.26	0.17	0.19
Al_2O_3	16.93	15.69	15.90	17.97	16.37	17.20	14.45	14.81	15.34	15.56	15.36
Fe_2O_3	0.88	1.41	1.20	2.77	1.64	2.35	0.70	1.84	1.30	0.64	0.78
FeO	1.21	1.36	1.25	3.18	1.41	3.42	1.21	1.44	1.37	1.15	1.18
MnO	0.03	0.05	0.03	0.08	0.04	0.08	0.02	0.06	0.03	0.04	0.05
MgO	0.64	0.69	0.38	2.69	0.71	2.15	0.25	0.75	0.40	0.29	0.34
CaO	3.18	1.60	1.53	4.84	3.37	3.57	1.52	2.10	1.60	1.71	1.77
Na_2O	4.02	4.12	2.75	4.63	4.14	4.07	3.19	3.45	3.40	4.15	3.98
K_2O	3.50	3.84	5.61	1.88	2.56	2.11	4.93	3.18	4.84	3.70	3.66
P_2O_5	0.12	0.11	0.10	0.31	0.16	0.17	0.06	0.11	0.08	0.08	0.08
H_2O^-	0.07	0.17	0.28	0.15	0.16	0.31	0.06	0.07	0.06	0.11	0.05
H_2O^+	0.35	0.76	0.48	0.95	0.25	1.02	0.17	0.44	0.46	0.24	0.16
Total	98.77	99.95	99.48	98.14	99.53	98.92	97.77	97.01	97.03	98.65	98.19
Qz	22.86	26.64	28.26	9.21	26.32	18.13	29.54	30.56	25.32	28.03	28.79
Or	20.68	22.69	33.14	11.11	15.12	12.47	29.12	18.79	28.59	21.86	21.62
Ab	34.00	34.85	23.26	39.16	35.01	34.42	26.98	29.18	28.76	35.10	33.66
An	15.00	7.22	6.94	22.00	15.68	16.61	7.15	9.70	7.42	7.96	8.26
Co	1.04	2.11	2.76	0.26	1.04	2.14	1.25	2.14	1.79	1.81	1.83
Hy En	1.59	1.72	0.95	6.70	1.77	5.35	0.62	1.87	1.00	0.72	0.85
Fs	1.01	0.96	0.80	2.53	0.55	3.25	1.43	0.53	1.07	1.38	1.30
Il	0.63	0.53	0.65	1.35	0.87	1.42	0.28	0.82	0.49	0.32	0.36
Mt	1.28	2.04	1.74	4.02	2.38	3.41	1.01	2.67	1.88	0.93	1.13
Ap	0.28	0.25	0.23	0.71	0.37	0.39	0.14	0.25	0.18	0.18	0.18
D.I.	77.54	84.18	84.66	59.48	76.45	65.02	85.64	78.53	82.67	84.99	84.07

Contents are in wt.%. D.I.; Differenciation index.

CIPW Norms. BCS No269 of British chemical standards were used for the wet analysis of SiO_2. The titration method with 1/20 N $KMnO_4$ was used to separate ferrous iron from total iron. The JG-la, JG-2, and JGb-l standards were used to determine the conversion factor of ferrous iron. Rare Earth Element results are given in parts per million, and are listed in Table 6. C.N. values (i.e. ppm value/ chondritic abundance) were obtained using chon-

Table 6-1. Rare earth element (12 elements) abundances of the granitic rocks.

Rock	Gneissose gd.(HGn)		Geochang gd.(Gc)		
Sample	H59	H105	H47	H102	H108
La	51.40	61.80	45.10	66.40	27.70
Ce	88.82	109.78	81.74	114.99	47.96
Pr	8.39	10.64	8.51	11.84	4.95
Nd	26.84	36.62	30.43	39.07	17.51
Sm	3.80	5.65	4.81	6.06	2.94
Eu	0.80	1.03	1.05	0.79	0.62
Gd	2.67	3.78	3.31	4.10	2.22
Dy	1.89	2.53	2.36	2.66	1.83
Ho	0.35	0.45	0.42	0.44	0.33
Er	1.05	1.22	1.24	1.11	0.96
Yb	0.97	0.83	1.14	0.98	0.84
Lu	0.18	0.13	0.18	0.17	0.13

Contents are in ppm. Abbreviations: Gc; Geochang granodiorite, HGn; Gneissose granodiorite, and gd.; granodiorite.

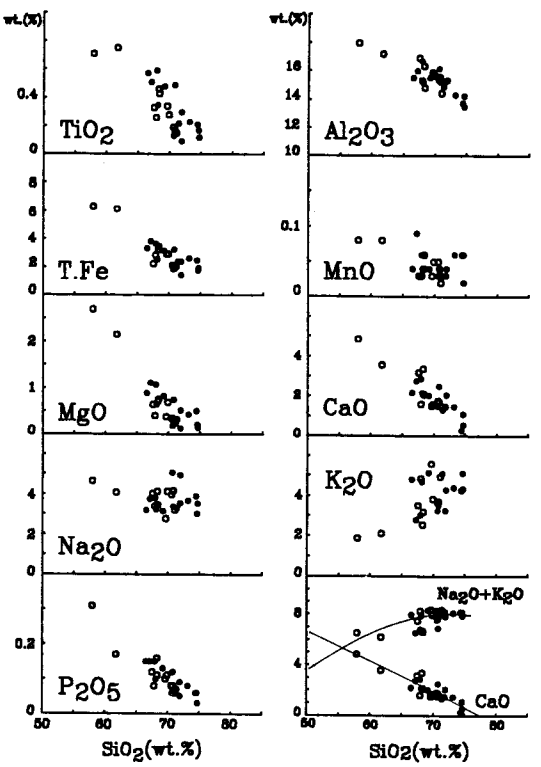

Fig. 6. SiO_2-Oxides variation diagram. Symbols are the same as those in Fig. 2.

Table 6-2. Rare earth element (7 elements) abundances of the granitic rocks.

Rock	Gneissose granodiorite (HGn)													
Sample	H1-1	H1-2	H3	H5	H8	H10	H19	H59	H62	H84	H88	H94	H104	H105
La	49.0	42.0	53.0	62.0	40.0	46.0	45.0	54.0	32.0	13.0	14.0	14.0	48.0	60.0
Ce	87.0	71.0	99.0	136.0	98.0	82.0	79.0	90.0	82.0	18.0	21.0	24.0	87.0	104.0
Nd	28.0	29.0	36.0	41.0	24.0	27.0	28.0	25.0	17.0	7.0	9.0	8.0	30.0	34.0
Sm	4.3	5.6	6.6	7.4	3.9	4.9	5.0	3.6	3.2	0.6	1.0	1.3	5.5	5.8
Eu	0.9	0.8	0.5	0.9	0.8	0.6	0.4	0.6	0.5	0.2	0.3	0.2	0.7	0.8
Dy	1.1	3.2	1.7	3.3	1.5	1.7	1.6	1.1	1.6	0.1	0.1	0.7	2.3	1.7
Yb	0.5	1.5	0.3	1.2	0.6	1.0	0.7	0.5	1.7	0.3	0.4	1.0	1.5	0.6
Rock	Geochang granodiorite (Gc)													
Sample	H17	H41	H44	H46	H47	H90	H101-2	H102	H103	H108	H110			
La	25.0	22.0	62.0	42.0	50.0	41.0	37.0	67.0	55.0	29.0	29.0			
Ce	38.0	40.0	115.0	70.0	87.0	71.0	66.0	112.0	99.0	48.0	50.0			
Nd	16.0	15.0	34.0	33.0	31.0	31.0	23.0	38.0	35.0	18.0	16.0			
Sm	2.0	2.3	5.6	6.0	5.5	5.5	4.5	6.4	6.5	3.1	2.9			
Eu	0.6	0.5	0.8	1.1	0.8	1.0	0.6	0.7	0.6	0.6	0.4			
Dy	0.4	0.9	1.2	3.2	1.8	4.2	1.3	2.1	2.3	0.9	0.6			
Yb	0.3	0.9	0.5	1.5	1.1	2.9	0.6	0.8	1.1	0.6	0.5			

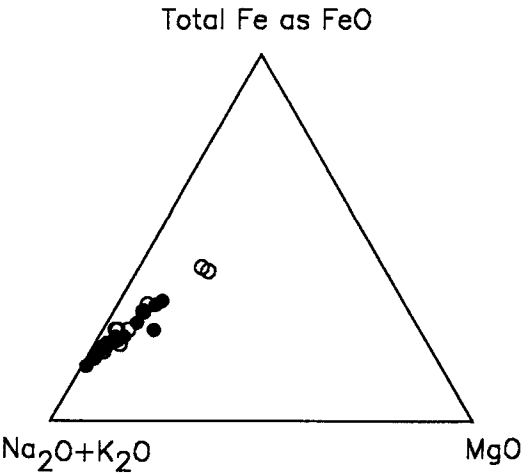

Fig. 7. AFM diagram of the granitic rocks. Symbols are the same as those in Fig. 2.

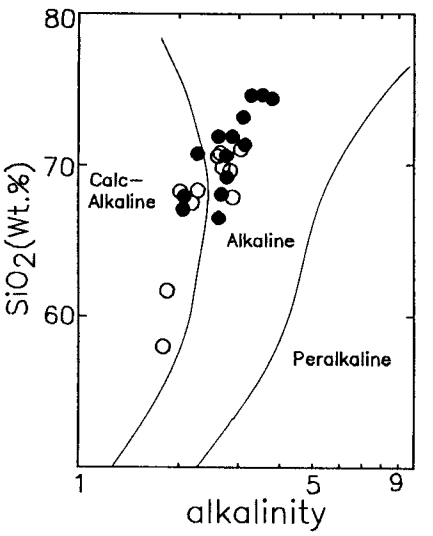

Fig. 8. Alkalinity ratio variation diagram for the granitic rocks.

dritic abundance data based on Nakamura (1974).

Major Elements

The SiO_2-Oxides diagram is shown in Fig. 6. The dots of the Geochang granodiorite and the Gneissose granodiorite show a continuous trend whose relation coefficient is relatively high. But the widely scattered contents of Na_2O, K_2O are against the above annotation. P_2O_5 content is higher in the Geochang granodiorite, which is coincident with the high content of apatite, in modal analysis. The content of metallic elements is generally higher in the Geochang granodiorite, which is in accord with the content of mafic minerals in modal analysis.

The intersection of two multiple regression lines in Fig. 6, $NK=-0.00093S^2-0.10965S+1.4158$ for Na_2O+K_2O and $C=-0.02489S^2+3.2884S-1.0613$ for CaO, represents 56 in alkali-lime index, which belongs to the calc-alkaline series near to the alkali-calcic rock series according to Peacock's criterion. Lee (1977) reported that the index was 66 in the Gyonggi massif, 62 in the Ogcheon zone, and 58 in the Gyeongsang basin.

The plots in the AFM diagram (Fig. 7) are traced as a differentiation path of a comagma suite with a nearly straight line. This concept of a comagma suite in the area is contrary to the results from mineral composition, zircon morphology, and REE pattern. The Gneissose granodiorite is rich in alkali, proving that the minerals of the rock were crystallized during a late magmatic period. The Gneissose granodiorite is also plotted in an alkaline area in Fig. 8, compared with the Geochang granodiorite.

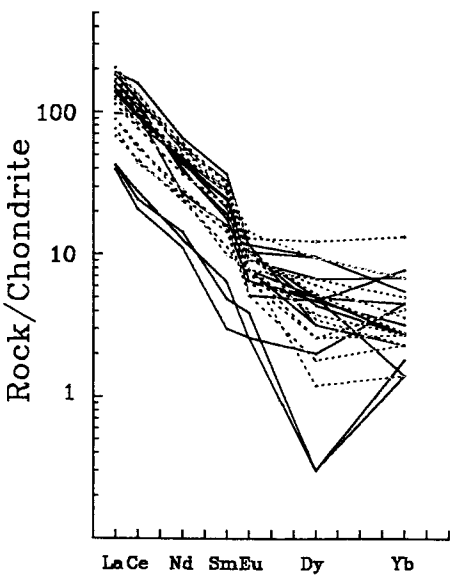

Fig. 9. Chondrite-normalized REE patterns for the granitic rocks. Dotted lines; the Geochang granodiorite and Solid lines; the Gneissose granodiorite.

Rare Earth Elements

The range of ΣREE is 81.6 to 227.0 pm in the

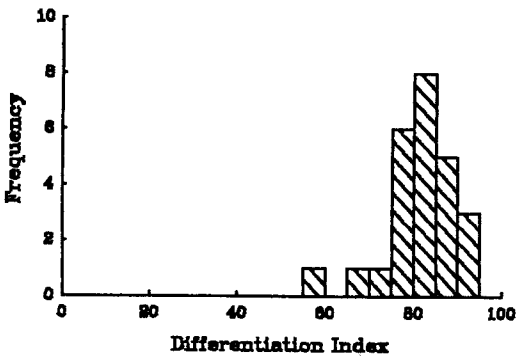

Fig. 10. Frequency distributions of differentiation index.

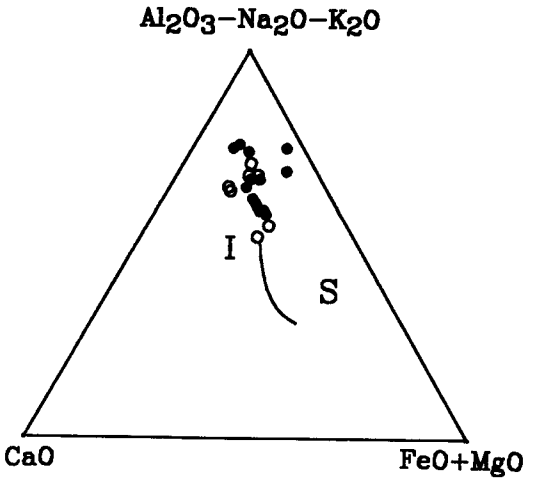

Fig. 11. ACF triangular diagram. S; S-type and I; I-type. Symbols are the same as those in Fig. 2.

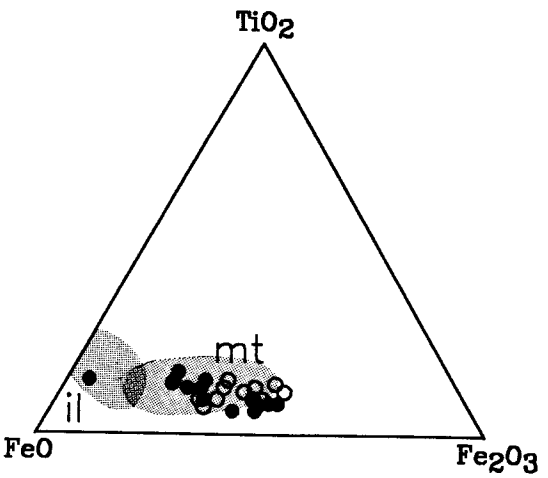

Fig. 12. TiO_2-FeO-Fe_2O_3 triangular diagram. il; ilmenite series and mt; magnetite series. Symbols are the same as those in Fig. 2.

Geochang granodiorite; 39.2 to 251.8 pm in the Gneissose granodiorite. The data of three samples is far apart from the mean value in the Gneissose granodiorite (Fig. 9). If the three samples are excepted, the range of ΣREE in the Gneissose granodiorite is limited to 138.0 to 251.8 ppm. The (La/Yb)cn of seven elements is 10 to 82 in the Geochang granodiorite, 13 to 115 in the Gneissose granodiorite, except for the three samples above. The ratio of twelve elements is 23 to 39 in the Geochang granodiorite 29 to 51 in the Gneissose granodiorite.

The origin of the tectonic setting can be induced from the LREE/HREE ratio. The REE pattern of some granitoids from continental or continent-margin setting has a large REE content (ΣREE=60−499 ppm, (La/Lu)cn=8.9−66, while those from the young island arc or the plagiogranodiorites from ophiolites have low REE contents (ΣREE=34−131 ppm, (La/Lu)cn =0.34−1.7) (Henderson, 1982). The LREE/HREE ratio also increases as the magma is differentiated. If the two granitic rocks were formed by a comagma suite, the ratio must be continuous. Also the Gneissose granodiorite has to be differentiated from the Geochang granodiorite, because the LREE/HREE ratio of the Geochang granodiorite is lower than that of the Gneissose granodiorite. The low LREE/HREE ratio and negative Eu anomalies require a formation by abundant plagioclase crystallization from less differentiated melts (Saunders et al., 1979). But if the two granitic rocks were formed by different magma suites, the Gneissose granodiorite may be intruded by the Geochang granodiorite. In this case, the anomalous three samples in the Gneissose granodiorite could be explained by ΣREE depletion due to any of several reasons, such as a metamorphism. The results in Fig. 2, 3, 5, and Fig. 9 support the later supposition (different origin), and the continuous trend in Fig. 3b, 6, and Fig. 7, the former one (comagma suite). Taking into account that a separate magma can also show a continuous trend in chemical composition, two magmatisms, different in temperature and chemical composition, could have coexisted in the area.

The granitoids show a negative correlation between REE content and differentiation index (DI). The absolute concentration range of each HREE is wider than that of LREE, suggesting that HREE were transported more readily in some fluids than the LREE by accessory minerals such as allanite

(LREE>>HREE) and/or zircon (HREE>>LREE). The mobility of the REE during magmatism can be presumed, taking into account the enrichment of La, Ce and Yb in the Gneissose granodiorite, the depletion of Yb in the Geochang granodiorite. Eu/Sm is 0.092 to 0.300 in the Geochang granodiorite, 0.075 to 0.209 in the Gneissose granodiorite, both of the granitic rocks show negative Eu anomalies. Negative Eu anomalies require a fractional crystallization model, from which much plagioclase is removed (Drury, 1978; Perfit et al., 1980).

Tectonic Setting and Type of Magma Source

Some chemical criteria to determine the tectonic setting of plutonic rock suites were proposed by Petro et al. (1979). They suggest that liquids in extensional areas are most likely to have been produced by melting of the small amounts of a relatively anhydrous peridotitic mantle, whereas liquids in compressional areas are produced by the melting of the subducted oceanic crust and overlying partially hydrated mantle.

The frequency distribution of the differentiation index (DI) show a unimodal pattern near 80 (Fig. 10). In alumina saturation type, the granitoids belong to also peraluminous rock which is $Al_2O_3>Na_2O+K_2O+CaO$. Both of the granitic rocks in the area belong to the compressional rock suite according to the above frequency distributions of DI, alumina saturation type, and the trend pattern on the AFM ternary diagram.

Some other parameters were also applied to determine the type of magma source which had formed the granitic rocks. Both granitic rocks are classified into the I-type group (Fig. 11) by Chappell and White (1974), or into the magnetite series (Fig. 12) by Ishihara (1977). There are many analogies in the mineralogical and chemical aspects between the I-type group and the magnetite series, so that these are often regarded as having a similar petrogenetic environment. I-type (or magnetite series) granitoids are thought to originate in the upper mantle or lowest crust, while S-type (or ilmenite series) granitoids are in the lower to middle crust. But several parameters, such as the normative corundom and the degree of alumina saturation, show a different interpretation for the grouping of the magma source in the area.

Another method was to use zircon form in order to justify the grouping. About a hundred zircon crystals were first separated from each rocks, and observed under a reflective microscope. Edge and corner of zircon crystals are sharp in I-type granitoids, partly eroded in S-type ones (Lee., 1990). The zircon crystals in the area have a sharp margin, while those from the pre-Cambrian Sobaegsan gneiss complex are eroded.

Thus the granitic rocks may be products of the magmatism connected with the Daebo orogeny and may originate not by a partial melting of water-deficient peridotitic mantle at greater depths, but by an alkali-calcic liquid which could be produced by the partial melting of the continental, subducted ocean crust or overlying partially hydrated mantle.

CONCLUSIONS

The granodiorites in the area were studied from the view point of rock forming mineralogy, zircon morphology, and petrochemistry.

The conclusions are as follows:

1. In the area, two magmatisms could be estimated, which differed in temperature and chemical composition, in activity with a similar formation age. But magmatism of a comagma suite cannot be excluded.
2. The granitic rocks can be divided into the Gneissose granodiorite and the Geochang granodiorite. Both are classified as granodiorite.
3. The granitic rocks belong to the calc-alkaline rock series and the I-type (magnetite series) rock suite. The rocks are interpreted to have originated in an calc-alkaline liquid which could be produced by the partial melting of the lowest crust or upper mantle.
4. The Geochang granodiorite shows the open scissors type in the PPEF diagram, which means a longer and slower crystallizing process in high to low temperature conditions and a more intermittent cooling history of water-rich magma than the Gneissose granodiorite.
5. The mean prism index of zircon crystals shows a relatively narrow range between 0.48 and 0.55 in the Gneissose granodiorite, but a wide range between 0.30 and 0.55 in the Geochang granodiorite. The zircon crystals in the Geochang granodiorite might have been mostly crystallized in a low temperature melt. The Gneissose granodiorite has {101}={211} pyramid, the Geochang granodiorite has both {101} dominant and {211} dominant in its zircon pyramid forms.

REFERENCES

Caruba, R., Baumer, A. and Turco, G. (1974) Nouvelles

syntheses hydrothermales du zircon. Geochim. Cosmochim. Acta, v. 39, p. 11-26.

Chappell, B.W. and White, A.J.R. (1974) Two contrasting granodiorite types, Pacific Geol., v. 8, p. 1/3-1/4.

Drury, S.A. (1978) REE distributions in a high-grade Archean gneiss complex in Scotland. Precambrian Res., v. 7, p. 237-257.

Hayashi, M. (1989) Quantitative description of zircon crystal forms. J. Min. Pet. Econ. Geol., v. 84, p. 152-158.

Hayashi, M. (1990) Zircon crystal morphology and its application to earth science. Jour. Geol. Soc. Japan, v. 96, p. 117-123.

Henderson, P. (1982) Inorganic Geochemistry. Pergamon, Oxford, p. 353.

Hine, R., Williams, I.S., Chappel, B.W. and White, A.J.R. (1978) Contrast between I-type and S-type granitoids of the Kosciusko batholith. J. Geol. Soc. Australia, v. 25, p. 219-235.

Ishihara, S. (1977) The magnetite-series and ilmenite-series granitic rocks. Min. Geol., v. 27, p. 293-305.

Karakida, Y. (1963) Classification and discrimination of crystal habits in zircons. Studies in Literature and Science, Seinan Gakuin University, v. 3, p. 77-86.

Kim, Y.J., Cho, D.L. and Park, Y.S. (1989) K-Ar ages and major mineral compositions of the Mesozoic igneous rocks in the vicinity of the Geochang area. J. Korean Inst. Min. Geol., v. 22, p. 117-127.

Lameyre, J. and Bowden, J. (1982) Plutonic rock types series. J. Geother. Res., v. 14, p. 169-186.

Lee, C.L. (1990) Zircon separation and its geological application, J. Taegu Education. v. 18, p. 149-156.

Lee, C.L., Lee, Y.J. and Hayashi, M. (1990) Petrology of the granitoids in the vicinity of Mt. Baegma-Unnam, southeast Kimchon, Korea, J. Geol. Soc. Korea. v. 26, p. 527-540.

Lee, D.S. (1977) Chemical composition of petrographic assemblage of igneous and related rocks in south Korea. J. Korea Inst. Min. Geol. v. 10, p. 75-92.

Lee, Y.J. (1980) Petrochemistry of granitic rocks from the Eonyang and Ulsan area. J. Korea Inst. Min. Geol., v. 13, p. 69-79.

Moorhouse, W.W. (1959) The study of rocks in thin section. Harper & Brothers, New York, p. 50-63.

Park, J.B., Kim, Y.J. and Kim, C.B. (1990) Petrochemical study on igneous rocks in the Hamyang area. Kyongnam, Korea. J. Korea Inst. Min. Geol., v. 23, p. 105-123.

Peacock, M.A. (1931) Classification of igneous rock series. J. Geol. v. 39, p. 54-67.

Perfit, M.R., Brueckner, H., Lawrence, J.R. and Kay, R. W. (1980) Trace element and isotopic variations in a zoned pluton and associated volcanic rocks. Unalaska Island, Alaska. Contrib. Mineral. Petrol., v. 73, p. 69-87.

Petro, W.L., Vogel, T.A. and Wilband, J.T. (1979) Major-element chemistry of plutonic rock suites from compressional and extensional plate boundaries. Chemical Geol., v. 26, p. 217-235.

Pupin, J.P. (1980) Zircon and granodiorite petrology. Contrib., Mineral, Petrol., v. 73, p. 207-220.

Pupin, J.P. (1985) Magmatic Zoning of Hercynian Granitoids in France based on Zircon Typology, Schweiz. Mineral, Petrogr. Mitt. v. 65, p. 29-56.

Saunders, A.D. and Tarney, J. (1979) The geochemistry of basalts from a backarc spreading center in the East Scotia Sea. Geochim. Cosmochim. Acta, v. 43, p. 555-572.

Streckeisen, A. (1976) To each Plutonic Rock its proper name. Ear. Sci. Rev., v. 12, p. 1-33.

Wedepohl, K.H. (1978) Handbook of geochemistry. Springer-Verlag Berlin Heidelberg, v. II/3, p. 26-A-10.

White, A.J.R. and Chappell, B.W. (1977) Ultra-metamorphism and granitoids genesis. Tectonophys., v. 43, p. 7-22.

Manuscript received 19 June 1992.

咸陽-居昌 地域, 쥬라기 花崗岩類의 岩石學的 硏究

李澈洛 · 李倫鐘 · 林正雄

요 약 : 본 역의 쥬라기화강암류는 "편마상화강암"과 "대보화강암"으로 분류 (1 : 250,000 전주도폭, 1973) 되어져 있으나, "대보화강섬록암"은 본 연구에서의 거창화강섬록암에 해당된다. 이들 화강섬록암류에 대한 조암광물의 경하기재, 암석화학, 및 저어콘의 형태적 연구를 하였다.

모드조성상 이들은 주로 화강섬록암에 해당되지만 편마상화강섬록암은 Trondhjemitic trend를, 거창화강섬록암은 granodioritic trend를 각각 따른다. 이들 두 암체는 모두 칼크-알칼라인 계열이며 I-type (자철석계열)에 속하나, 편마상화강섬록암은 분화말기에 La, Ce, Yb의 enrichment를 겪은 반면, 거창화강섬록암은 분화초기에 Yb의 depletion을 겪은 것으로 생각된다.

사장석은 대체로 올리고클레이스에 해당한다. 흑운모는 (Mg, Fe) 고용체간의 성분변화보다 (Si, Al) 고용체간의 변화가 더 뚜렷하다. 각섬석은 거창화강섬록암에서만 제한적으로 산출되며 tschermakite에 해당한다. 저어콘 주면의 상대적 발달을 보면, 편마상화강섬록암은 대부분 {100}={110}형에 가까운 것들이 많으나, 거창화강섬록암은 {110} 탁월형 (저온형)에서 {100} 탁월형 (고온형)에 이르는 다양한 변화를 보인다. 그러나 이들은 대부분 저온형 마그마 용체내에서 결정화되었다. PPEF (Prism-Pyramid-Elongation-Flatness) 도에서, 편마상화강섬록암은 닫힌 가위형 (closed scissors type), 거창화강섬록암은 열린 가위형 (open scissors type)을 보인다. 이는 거창화강섬록암의 저어콘들이 지각물질 또는 편마상화강섬록암을 형성시킨 잔류마그마와 혼화된 마그마로부터 정출되었음을 암시해 주는 것으로 생각된다.